Journal of Experimental Botany, Vol. 64, No. 2, pp. 599–612, 2013
doi:10.1093/jxb/ers352 Advance Access publication 10 December, 2012
This paper is available online free of all access charges (see http://jxb.oxfordjournals.org/open_access.html for further details)

Journal of Experimental Botany
www.jxb.oxfordjournals.org

RESEARCH PAPER

Partial deficiency of isoleucine impairs root development and alters transcript levels of the genes involved in branched-chain amino acid and glucosinolate metabolism in *Arabidopsis*

Hailan Yu[1], Fengxia Zhang[2], Guodong Wang[2], Yule Liu[1] and Dong Liu[1,*]

[1] MOE Key Laboratory of Bioinformatics, School of Life Sciences, Tsinghua University, Beijing 100084, China
[2] State Key Laboratory of Plant Genomics and National Plant Gene Research Center, Institute of Genetics and Developmental Biology, Chinese Academy of Sciences, Bejing 100101, China

* To whom correspondence should be addressed. E-mail: liu-d@mail.tsinghua.edu.cn or dongliu64@yahoo.com

Received 8 October 2012; Revised 7 November 2012; Accepted 9 November 2012

Abstract

Isoleucine is one of the branched-chain amino acids (BCAAs) that are essential substrates for protein synthesis in all organisms. Although the metabolic pathway for isoleucine has been well characterized in higher plants, it is not known whether it plays a specific role in plant development. In this study, an *Arabidopsis* mutant, *lib* (*low isoleucine biosynthesis*), that has defects in both cell proliferation and cell expansion processes during root development, was characterized. The *lib* mutant carries a T-DNA insertion in the last exon of the *OMR1* gene that encodes a threonine deaminase/dehydratase (TD). TD catalyses the deamination and dehydration of threonine, which is the first and also the committed step in the biosynthesis of isoleucine. This T-DNA insertion results in a partial deficiency of isoleucine in *lib* root tissues but it does not affect its total protein content. Application of exogenous isoleucine or introduction of a wild-type *OMR1* gene into the *lib* mutant can completely rescue the mutant phenotypes. These results reveal an important role for isoleucine in plant development. In addition, microarray analysis indicated that the partial deficiency of isoleucine in the *lib* mutant triggers a decrease in transcript levels of the genes encoding the major enzymes involved in the BCAA degradation pathway; the analysis also indicated that many genes involved in the biosynthesis of methionine-derived glucosinolates are up-regulated.

Key words: Branched-chain amino acid, glucosinolate, metabolism, isoleucine deficiency, root development, threonine deaminase/dehydratase, transcript levels.

Introduction

Characterized by their small, branched, hydrocarbon residues, leucine, isoleucine, and valine together form a unique group of so-called branched-chain amino acids (BCAAs). Humans and animals cannot synthesize these three amino acids and must obtain them from other sources, such as plants. In plants, some enzymes involved in BCAA biosynthesis are the

Abbreviations: AHAS, acetohydroxyacid synthase; BCAA, branched-chain amino acid; BCAT, branched-chain aminotransferase; CaMV, *Cauliflower mosiac virus*; BCKDH, branched-chain α-keto dehydrogenase; DHAD, dihydroxyacid dehydratase; GAPCps, plastidial GAPDH; GAPDH, glyceraldehyde-3-phosphate dehydrogenase; IPMS, isopropylmalate synthase; KARI, ketol acid reductoisomerase; IVD, isovaleryl-CoA dehydrogenase; LRC, long root cell; MCCase, 3-methycrotonyl-CoA carboxylase; MS, Murashige and Skoog; QC, quiescent centre; SRC, short root cell; TAIL-PCR, thermal asymmetric interlaced PCR; TD, threonine deaminase/dehydratase.

targets of several herbicides. Because of their importance in human and animal nutrition and agriculture, the biosynthesis pathways of BCAAs in higher plants have been extensively studied and well characterized (Singh and Shaner, 1995; Binder, 2010).

In plants, the conversion of threonine to 2-oxobutanoate is the first and also the committed step towards isoleucine biosynthesis. This reaction is catalysed by threonine deaminase/dehydratase (TD) (Fig. 7A). After four more enzymatic reactions, 2-oxobutanoate is condensed with one molecule of pyruvate and subsequently transformed into isoleucine. A unique feature of BCAA biosynthesis in plants is that the four enzymes that catalyse the reactions for production of isoleucine are also used for biosynthesis of valine starting from the condensation of two molecules of pyruvate. These four enzymes, acetohydroxyacid synthase (AHAS), ketol acid reductoisomerase (KARI), dihydroxyacid dehydratase (DHAD), and branched-chain aminotransferase (BCAT), act in parallel on different substrates and finally lead to the production of isoleucine and valine. The last intermediate of valine biosynthesis, 3-methyl-2-oxobutanoate, is also the initial substrate in the branch leading to leucine biosynthesis. Through four enzymatic reactions, this substrate is converted to leucine, with the first step catalysed by isopropylmalate synthase (IPMS) (Fig. 7A). For all three BCAAs, the enzymes involved in the last step of production are BCATs. BCATs also catalyse the first step of BCAA degradation (Fig. 7B). Interestingly, some enzymes involved in leucine biosynthesis are also used for synthesis of glucosinolates through the methionine chain elongation pathway (Sønderby *et al.*, 2010).

In plants, BCAA homeostasis is strictly regulated. So far, our understanding of such regulation comes mostly from the studies of allosteric control of three enzymes, namely TD (Halgand *et al.*, 2002), AHAS (McCourt and Duggleby, 2006), and IPMS (de Kraker *et al.*, 2007). It is well known that the activity of TD is feedback inhibited by its end-product, isoleucine. An *Arabidopsis* mutant with a feedback-insensitive TD overaccumulates isoleucine (Mourad and King, 1995). The feedback inhibition of TD by isoleucine is antagonized by valine. Similarly, AHAS is inhibited by each of the BCAAs, and IPMS is feedback regulated by leucine. It remains unclear, however, whether other regulatory mechanisms control BCAA homeostasis. For example, it is not known whether a deficiency of a particular BCAA will affect transcript levels of the genes involved in the BCAA metabolic pathways.

In humans and other animals, some amino acids serve not only as building blocks for protein synthesis but also as signals that control gene transcription, translation of mRNAs, and metabolic activities (Meijer and Dubbelhuis, 2004; Kimball and Jefferson, 2006). For example, leucine plays an important role in the regulation of autophagy, which is associated with many physiological processes, such as development, cell death, and tumour suppression (Levine and Klionsky, 2004). Whether leucine has a similar function in plants is unclear. Previous studies have shown that homeostasis of some amino acids may also have regulatory functions in sustaining plant root growth and development. Glyceraldehyde-3-phosphate dehydrogenase (GAPDH) catalyses the conversion of glyceraldehyde-3-phosphate to 1,3-bisphosphoglycerate. The plastidial GAPDH (GAPCps) has two isoforms in *Arabidopsis* (GAPCp1 and GAPCp2), which are important for the synthesis of serine in roots (Muñoz-Bertomeu *et al.*, 2009). The *gapcp* double mutant, which contains reduced levels of serine in roots and aerial parts, displays a drastic phenotype of arrested root development. All these mutant phenotypes can be rescued by exogenously applied serine. The homeostasis of another amino acid, histidine, also affects root development. The *Arabidopsis* mutant *hpa1*, which has a 30% reduction in free histidine content, has a very short root system and exhibits a specific defect in root meristem maintenance (Mo *et al.*, 2006). Similarly, its mutant phenotype can be fully rescued by exogenously applied histidine or by introduction of a wild-type (WT) functional *HPA1* gene. The effect of perturbed histidine homeostasis on plant development was also observed for the *Arabidopsis* mutant *apg10* (Noutoshi *et al.*, 2005). In addition, exogenously applied glutamate can act as a signal to modulate primary root growth and lateral root formation, probably through the interaction with the auxin signalling pathway (Walch-Liu *et al.*, 2006). Whether the three BCAAs play any specific roles in regulating plant development is currently unknown.

In this work, an *Arabidopsis* mutant called *lib* (*low isoleucine biosynthesis*) that showed severe defects in root development was identified. Genetic and molecular analysis indicated that the mutant phenotype is caused by a T-DNA insertion within the *OMR1* gene, which encodes a threonine deaminase/dehydratase (TD). As a consequence, the mutant produces less isoleucine than the WT. Furthermore, it was found that the partial deficiency of isoleucine in *lib* alters transcript levels of the genes encoding the enzymes involved in BCAA and glucosinolate metabolic pathways.

Materials and methods

Plant materials and growth conditions

Arabidopsis seeds were surface sterilized with 20% (v/v) commercial bleach for 20 min, followed by four washes in sterile distilled water. The sterilized seeds were then sown on Petri dishes containing a medium of half-strength Murashige and Skoog (MS) basal salts with 1% sucrose, 0.1% MES (adjusted to pH 5.7 with 1 N NaOH), and 1.2% agar. After 2 d of stratification at 4 °C, the agar plates were placed vertically in the growth room with a photoperiod of 16 h light:8 h dark at 22–24 °C. The light intensity was 100 μmol m^{-2} s^{-1}.

Mutant isolation

The seeds of an *Arabidopsis* T-DNA activation tagging library (Qin *et al.*, 2003) were directly sown on Petri dishes containing half-strength MS medium as described above. At 8 days after seed germination (DAG), the seedlings with short primary roots were selected and transferred to soil. The progeny from self-pollinated plants were retested for their root growth phenotype. The confirmed root mutant was backcrossed to the WT three times before further characterization. The genetic linkage between the mutant phenotype and T-DNA insertion was tested by growing the segregated F_2 progeny from the backcross on half-strength MS medium supplemented with glufosinate ammonium (Basta) (20 μg ml^{-1}).

Histochemical staining for GUS activity

The histochemical analysis of β-glucuronidase (GUS) activity was performed as described (Jefferson *et al.*, 1987).

Microscopy

For light microscopy, the excised roots or whole seedlings collected at different stages after germination were mounted in HCG clearing solution (30 ml of H_2O, 80 g of chloral hydrate, 10 ml of 100% glycerol) and examined with a differential interference contrast (DIC) microscope (Olympus BX51, Japan) or stereomicroscope (Olympus SZ61, Japan).

Eight-day-old WT and *lib* seedlings carrying the markers SCR–GFP (green fluorescent protein), J0571–GFP, CS9227–GFP, CS9093–GFP, WOX5–GFP, and PLT1–CFP (cyan fluorescent protein) were used for confocal microscopic analysis. The roots were excised from the seedlings and stained with 10 μM propidum iodide (PI) for 5 s, and rinsed with distilled water. The specimens were examined with a confocal laser scanning microscope (Zeiss 710META, Germany). Excitation wavelengths of 546, 488, and 433 nm were used to visualize the signals of PI staining, GFP, and CFP, respectively. The emission wavelengths were 573, 507, and 476 nm.

Determination of root meristem size and root cell length

To determine the root meristem size, the root tips were excised from seedlings at different developmental stages and examined with a DIC microscope. For the measurement of the lengths of epidermal cells, the roots excised from 8-day-old seedlings were stained with PI for 5 s and observed with a DIC florescence microscope (Olympus BAX51, Japan).

Cloning of T-DNA flanking sequence

The T-DNA flanking sequence in the *lib* mutant was cloned by thermal asymmetric interlaced PCR (TAIL-PCR) (Liu *et al.*, 1995). The authenticity of the cloned sequence was confirmed by PCR using two pairs of primers. The first pair comprised a primer within the T-DNA left border (5'-TTGACCATCATACTCATTGCTG-3') and a primer located at the sixth exon of the *OMR1* gene (5'-GGACCAATGAACATAAGCGA-3'); the second pair comprised two primers surrounding the T-DNA insertion site with the sequence 5'-GGACCAATGAACATAAGCGA-3' and 5'-GAAACCAAAAGGTAACCCAC-3'.

Vector construction and plant transformation

The detailed protocols for vector construction and plant transformation are described in Supplementary Text S1 available at *JXB* online.

Enzymatic activity assays for plant threonine deaminase/dehydratase

The detailed protocol for the plant TD enzymatic activity assay is described in Supplementary Text S1 at *JXB* online.

Quantitative real-time PCR analysis

Total RNAs were extracted from root and shoot tissues with the Tiangen RNAeasy kit (Tiangen, Beijing). DNase-treated RNA (1 μg) was reverse transcribed in a 20 μl reaction using M-MLV reverse transcriptase according to the manufacturer's manual (TaKaRa, Kyoto, Japan). cDNA was amplified using SYBR Premix Ex Taq (TaKaRa, Japan) with the Bio-Rad CFX96 real-time PCR detection system. The amounts of PCR products in each sample were normalized using the *ACTIN* gene as the internal control. The primers used for OMR1 amplification were: P1 (5'-GAAAGATCACCTGCGTTACTTGA-3'), P2 (5'-GGCATAGAACCTCGTCTCCA-3'), P3 (5'-GTTTGAAGCTGTGGTGGATAATC-3'), and P4 (5'-CTAAAACGCTCATCCGACAG-3').

The sequences of the primers used for amplification of other three genes were as follows: At5g23010, 5'-GAAATTGAACGCTGTCTTCTCA-3' and 5'-CGCTAGATGTTACTAATGCCTTCA-3'; At5g23020, 5'-CCGTGAACAGTGTTAAGTACGC-3' and 5'-CACCCGCTTTTATCGATTCT-3'; and At3g19710, 5'-CGCAACCTCTTCCTGTGAGT-3' and 5'-TCCGTACGAACAAACTTGAATG-3'.

Measurement of free amino acid content

Root tissue (100 mg) of 8-day-old *Arabidopsis* seedlings was ground into a fine powder in liquid nitrogen. A 300 μl volume of 80% ethanol was added to the powder, mixed well, and incubated for 30 min at 45 °C. The samples were then centrifuged at 12,000 rpm for 5 min to remove cell debris. The supernants were passed through a 0.22 μm filter into new sterile tubes. The chlorophyll was removed from the supernatants by extraction with cyclohexane. The supernatants were concentrated to 80 μl through vacuum evaporation and were analysed for free amino acid contents with a 1100 HPLC (HP, USA) amino acid analyser.

Total protein determination

The contents of total proteins of shoots and roots were determined according to Jing *et al.* (2009).

Microarray analysis

The microarray experiments were performed at ShanghaiBio Corporation. Total RNA was isolated using the RNase kit (Qiagen) from three replicate samples of the root tissues of 8-day-old WT and *lib* seedlings grown on half-strength MS medium. Total RNA was amplified, labelled, and purified with the GeneChip 3'IVT Express Kit (Cat#901229, Afftnetrix, Santa Clara, CA, USA) following the manufacturer's instructions to obtain biotin labelled cRNA. Array hybridization and wash were performed using the GeneChip® Hybridization, Wash and Stain Kit (Cat#900720, Affymetrix) in a Hybridization Oven 645 (Cat#00-0331-220V, Affymetrix) and Fluidics Station 450 (Cat#00-0079, Affymetrix) following the manufacturer's instructions. Hybridized slides were scanned by GeneChip©Scanner 3000 (Cat00-00212, Affimetrix) and Command Console Software 3.1 (Affymetrix) with default settings. Raw data were normalized by the MAS 5.0 algorithm, Gene Spring Software 11.0 (Agilent Technologies, Santa Clara, CA, USA). Microarray data analysis was performed using the SBC Analysis system, which is available on the website: http://sas.ebioservice.com/index.jsp. The username and password to access this website are available upon request. A general description of the SBC analysis system can be found on the website: http://www.ebioservice.com/eng/index.asp.

The microarray data generated in this study have been deposited in the Gene Expression Omnibus (GEO) database under the accession number GSE42060.

Statistical analysis

The two-sample *t*-test function of Origin software (OriginLab Corporation, Northampton, USA) was used for statistical analysis in this work.

Results

Identification of the lib *mutant*

A mutant, designated *lib* (*low isoleucine biosynthesis*), was identified from a T-DNA activation tagging library (Qin *et al.*, 2003). When grown on half-strength MS medium,

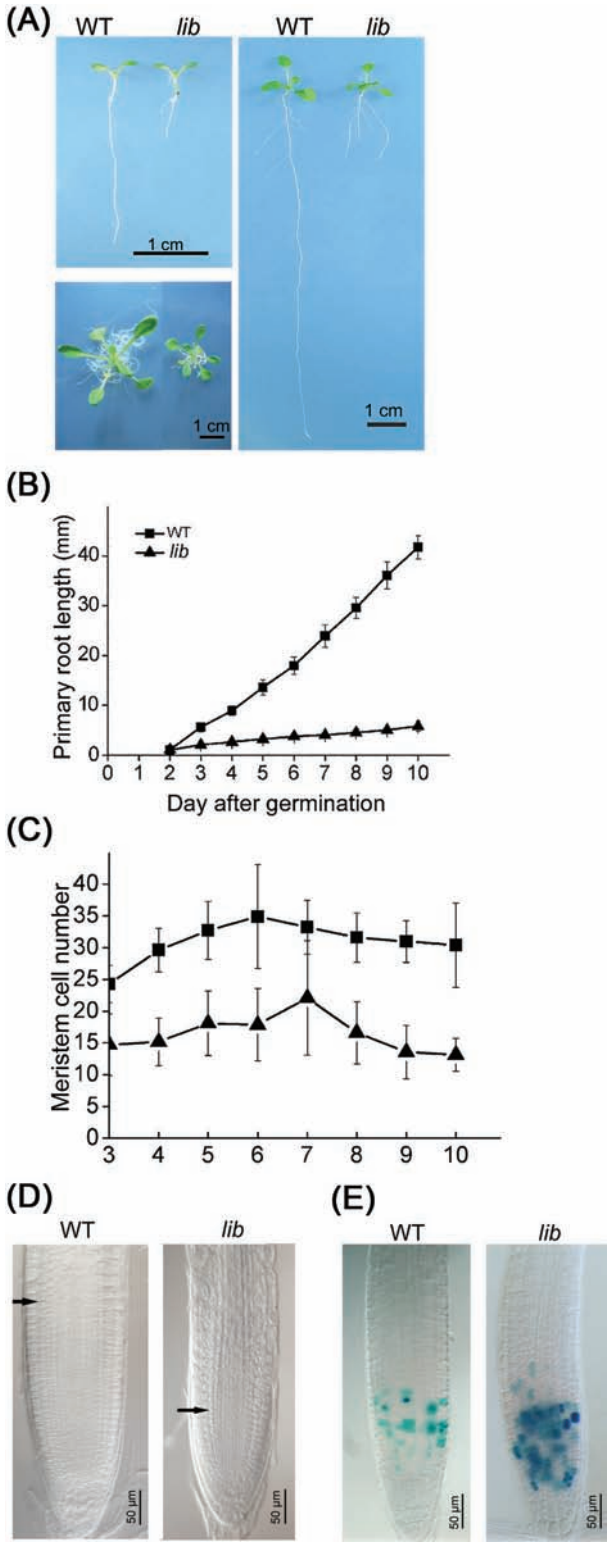

Fig. 1. Characteristics of growth of the WT and *lib* mutant. (A) Appearance of the WT and *lib* seedlings grown on half-strength MS medium at 7 (left upper panel), and 14 (right panel) days after germination (DAG). Left lower panel: appearance of shoots of WT and *lib* plants grown on half-strength MS medium for 21 d. (B) Changes in primary root length of the WT and *lib* mutant from 2 to 10 DAG. (C) Number of root meristem cells of the WT and *lib* mutant, measured over time from 3 to 10 DAG. In B and C, values are means ±SE (n >20). (D) Root meristematic zone of 8-day-old WT and *lib* mutant seedlings. Black arrows indicate the boundary between the root meristematic and elongation zones. (E) Expression of *CycB1::GUS* in the meristematic zones of 8-day-old WT and *lib* mutant seedlings.

lib had an abnormally short primary root (Fig. 1A). Time-course studies indicated that the short-root phenotype of *lib* was due to its low growth rate rather than to growth arrest at a certain developmental stage (Fig. 1B). Lateral roots became visible 5 DAG for *lib* but 8 DAG for the WT. Lateral root number, however, increased more rapidly for the WT than for the *lib* mutant; at 13 DAG, the WT had more lateral roots than the *lib* mutant (Supplementary Fig. S1 at *JXB* online). When seedlings were grown on half-strength MS medium for 21 d, shoots were significantly smaller for *lib* than for the WT (Fig. 1A). When grown in soil, however, no morphological differences were observed between *lib* and the WT (data not shown). In this research, a detailed analysis of the defects in root development of the *lib* mutant was conducted.

The lib *mutation impairs both cell division and expansion*

Root growth is a coordinated process of cell division and expansion. To investigate which process was affected in the *lib* mutant, its cell division activity was first examined. Because cell division activity in roots is reflected by the size of the root meristem, meristem sizes in WT and *lib* roots were compared by counting the number of cortex cells in a file extending from the quiescent centre (QC) to the first elongated cell. In the first 10 DAG, the meristem was 40–60% smaller in *lib* roots than in WT roots (Fig. 1C, D). To determine the cause of the low cell division activity in *lib*, the marker gene *CycB1::GUS* was introduced into *lib* through a genetic cross. Expression of the *CycB1::GUS* marker gene specifically occurs at the transition stage from the G_2 to M phase (Colón-Carmona *et al.*, 1999). The number of meristem cells expressing *CycB1::GUS* was greater in *lib* than in the WT (Fig. 1E). These results indicated that low cell division activity in *lib* was due to the slower transition of cells from the G_2 to M phase.

To determine whether the *lib* mutation also affects cell expansion, the size of root epidermal cells in *lib* and the WT was compared. In the root maturation zone of the WT, the epidermal cells were long and rectangular, and their lengths were relatively consistent (Fig. 2A). In the *lib* mutant, however, regions with short rectangular cells [referred to as long root cells (LRCs)] and regions with nearly square cells [referred to as short root cells (SRCs)] alternated (Fig. 2A, B). In an 8-day-old *lib* seedling, two regions with LRCs and two regions with SRCs were evident (Fig. 2B). The LRCs and SRCs in the *lib* mutant were 40% and 80% shorter, respectively, than the epidermal cells in the WT (Fig. 2D). Root hair cells were uniformly distributed along the primary root of the WT, but were unequally distributed in *lib* (Fig. 2C). In ~80% of 8-day-old *lib* seedlings, there were two segments on the primary root, which had few or no root hairs (Supplementary Fig. S2 at *JXB* online). These segments usually appeared at

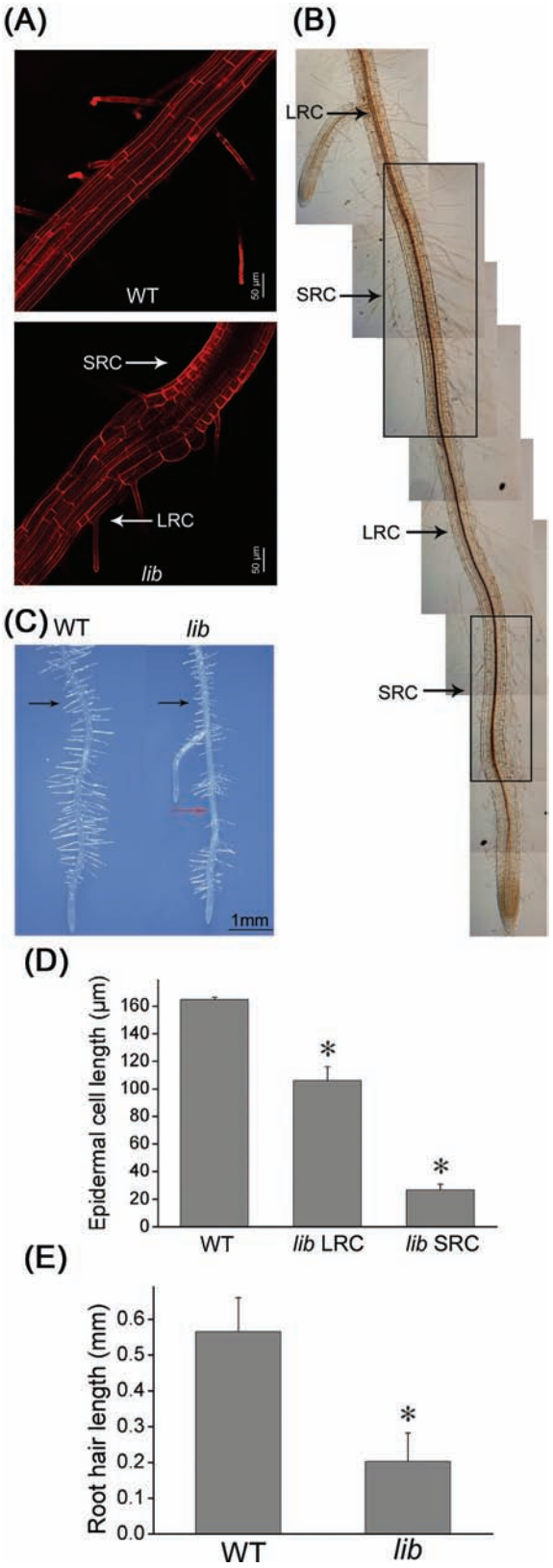

Fig. 2. Length of root epidermal cells and patterns of root hairs of the WT and *lib* mutant. (A) Lengths of root epidermal cells in the maturation zone of the WT and the *lib* mutant. The roots were stained with propidium iodide (PI) and photographed with a confocal microscope. In the mutant, the regions with long (LRCs) and short (SRCs) root cells are indicated by white arrows. (B) The relative positions of the regions with LRCs and SRCs (boxed) along the primary root of an 8-day-old *lib* seedling; LRCs and SRCs are indicated by black arrows. (C) The patterns of root hairs of 8-day-old WT and *lib* mutant seedlings. The black arrows indicate regions with continuous formation of root hairs, and the red arrow indicates a region lacking root hairs. (D) Root cell length in maturation zones of 8-day-old WT and *lib* mutant seedlings. *lib* LRC, the long root cells of the *lib* mutant; *lib* SRC, the short root cells of the *lib* mutant. Values are the means ±SE of 30 seedlings (10 root epidermal cells were measured per seedling). (E) Length of root hairs of 8-day-old WT and *lib* mutant seedlings. Values are the means ±SE of 30 seedlings (20 root hairs were measured per seedling). Asterisks indicate a significant difference according to a two-sample *t*-test ($P < 0.05$).

the junction between LRCs and SRCs. The length of the segments that had few or no root hairs varied among the *lib* roots examined. The length of the root hairs in the maturation zone was also compared. Overall, *lib* root hairs were ~70% shorter than WT root hairs (Fig. 2E). These results indicated that both cell proliferation and cell expansion were impaired in the *lib* mutant.

The lib *mutant has normal cell patterning*

To examine whether the cell patterning in the roots of the *lib* mutant was altered, the mutant was crossed to transgenic lines that carried various cell type-specific markers with GFP as a reporter gene. These marker lines included SCR–GFP (endodermis specific), J0571 (cortex and endodermis specific), CS9093 (epidermis specific), and CS9227 (columella specific) (http://www.plantsci.cam.ac.uk/Haseloff). Expression patterns of the marker genes did not differ significantly between the *lib* and WT plants, indicating that the *lib* mutation did not change the cell patterning in roots (Supplementary Fig. S3 at *JXB* online). To investigate whether the *lib* mutation affects the activity of the QC, which is responsible for maintaining the functions of root stem cells, the expression patterns of three marker genes were examined. QC46–GUS and WOX5–GFP are specifically expressed in QC cells, and PLT1–CFP is expressed only in the stem cell niche. Again, the expression of these three marker genes did not differ significantly between *lib* and the WT, suggesting that the *lib* mutation did not interfere with the functions of the QC and stem cell activity (Supplementary Fig. S3).

The lib *phenotype is caused by the insertion of a T-DNA into the* OMR1 *gene*

To find the molecular lesion responsible for the mutant phenotype, the *lib* mutant was backcrossed to the WT with the same ecotype background. The phenotype of all the F_1 plants was similar to that of the WT. Among the F_2 progeny, the ratio of plants with the mutant phenotype to the WT phenotype was ~1:3 (84:210), indicating that the mutant phenotype was caused by a monogenic recessive mutation. Further

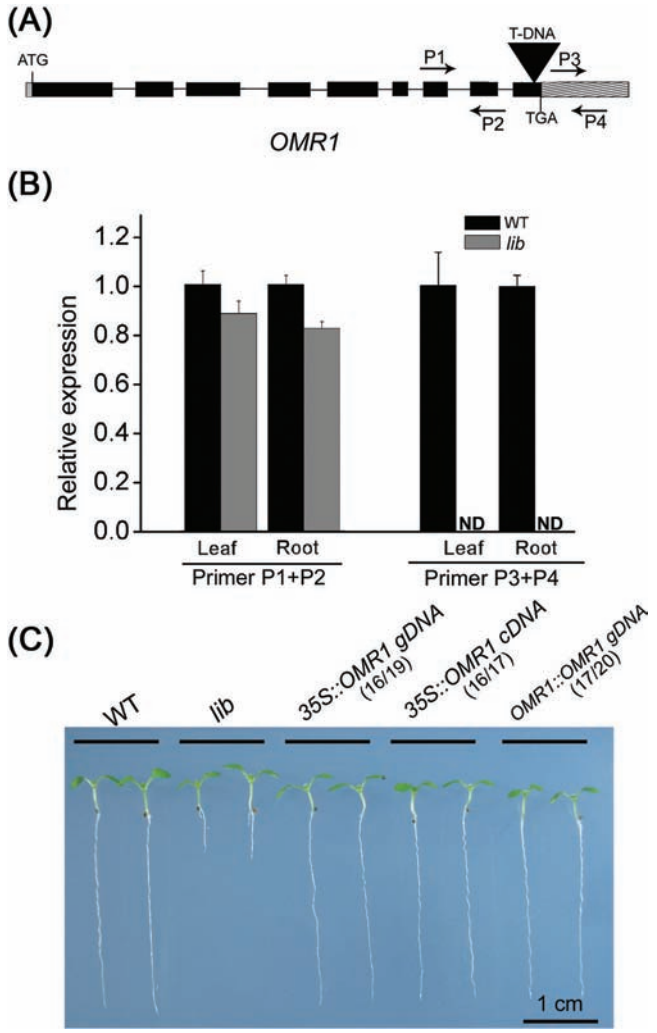

Fig. 3. T-DNA insertion in the *OMR1* gene and its effect on *OMR1* expression in the *lib* mutant. (A) Diagram showing the relative position of the T-DNA insertion (black triangle) in the *OMR1* gene of the *lib* mutant. The black box, grey box, and the horizontal line between the boxes represent the exons, untranslated regions, and introns, respectively. The positions of start (ATG) and stop (TGA) codons and two pairs of primers (P1, P2 and P3, P4) for real-time PCR analysis are shown. (B) The relative expression level of the *OMR1* gene in leaves and roots as determined by real-time PCR. ND, not detected. (C) Genetic complementation of the *lib* mutant. The photograph shows 10-day-old seedlings of the WT, *lib* mutant, and plant lines transformed with constructs of *35S::OMR1* (gDNA), *35S::OMR1* (cDNA), and *OMR1::OMR1* (gDNA). The numbers in parentheses indicate the number of independent transgenic lines with rescued phenotypes over the total number of transgenic lines obtained for each construct.

analysis showed that, in F_2 progeny, all the *lib* mutant plants were Basta resistant, whereas WT plants showed both Basta-resistant and Basta-sensitive phenotypes. These results suggested that the *lib* mutant phenotype is linked to the T-DNA insertion. Using the TAIL-PCR technique, it was found that the T-DNA was inserted into the last exon of the *OMR1* gene (At3g10050) (Fig. 3A). The *OMR1* gene encodes a TD that catalyses the deamination and dehydration of threonine, which is the first and also the committed step in the biosynthesis of isoleucine (Binder, 2010). The *OMR1* gene was first identified in an *Arabidopsis* mutant (*omr1-1*) that was resistant to the inhibition of the isoleucine structural analogue L-*O*-methylthreonine (Mourad and King, 1995). The *omr1-1* mutant produces an active but isoleucine feedback-insensitive form of TD because of two point mutations in the OMR1 protein. Plants with this mutation produce 20 times more isoleucine than the WT (Mourad *et al.*, 2000). Two pairs of primers were used in real-time PCR analysis to examine the expression level of the *OMR1* gene in the WT and *lib* mutant (Fig. 3A). With the primers P1 and P2, which are located within the seventh and eighth exons (before the T-DNA insertion), a similar amount of *OMR1* transcripts between these two primers was detected in both leaves and roots of the WT and *lib* (Fig. 3B). When primers P3 and P4, which amplify a region immediately after the T-DNA insertion, were used for real-time PCR analysis, no *OMR1* transcripts were detected in either shoots or roots of the *lib* mutant. The insertion of the T-DNA sequence also introduced two consecutive stop codons immediately at the insertion site, which caused a truncation of 13 amino acids at the C-terminus of the OMR1 protein. Because the expression level of the part of OMR1 mRNA before the T-DNA insertion site in *lib* is similar to that of the OMR1 mRNA in the WT (Fig. 3B), the mutant phenotype is probably caused by the truncation of the OMR1 proteins rather than by the blocked expression of the part of OMR1 mRNA after the T-DNA insertion site.

To confirm that the T-DNA insertion in *OMR1* was responsible for the *lib* mutant phenotype, the genomic and cDNA sequences of the WT *OMR1* gene were introduced back into *lib* mutant plants under the *Cauliflower mosaic virus* (CaMV) 35S promoter or *OMR1*'s own promoter. The restoration of *OMR1* gene expression to the level in the WT or overexpression of the *OMR1* gene was confirmed in roots of three independent transgenic lines for each construct (Supplementary Fig. S4 at *JXB* online). Analysis of the transgenic plants indicated that all three gene constructs, namely *35S::OMR1* [genomic DNA (gDNA)], *35S::OMR1* (cDNA), and *OMR1::OMR1* (gDNA), could restore the mutant phenotype of primary root growth (Fig. 3C). The other root growth parameters of an *OMR1::OMR1* (gDNA) line were then compared with those of the WT in terms of the size of the root meristem (Fig. 4A, B), length of epidermal cells (Fig. 4C), and length of root hairs (Fig. 4D). The defects in all root growth parameters examined for *lib* were rescued in the complemented line. These results demonstrated that the T-DNA insertion into the *OMR1* gene was indeed the cause of the *lib* mutant phenotypes.

Isoleucine biosynthesis is reduced in the lib *mutant*

Because the *lib* mutant expresses a truncated version of the *OMR1* gene, investigations were carried out to determine whether this would affect the total enzyme activity of TD. Total soluble proteins were extracted from 24-day-old WT and *lib* seedlings, and their TD activities were compared. The

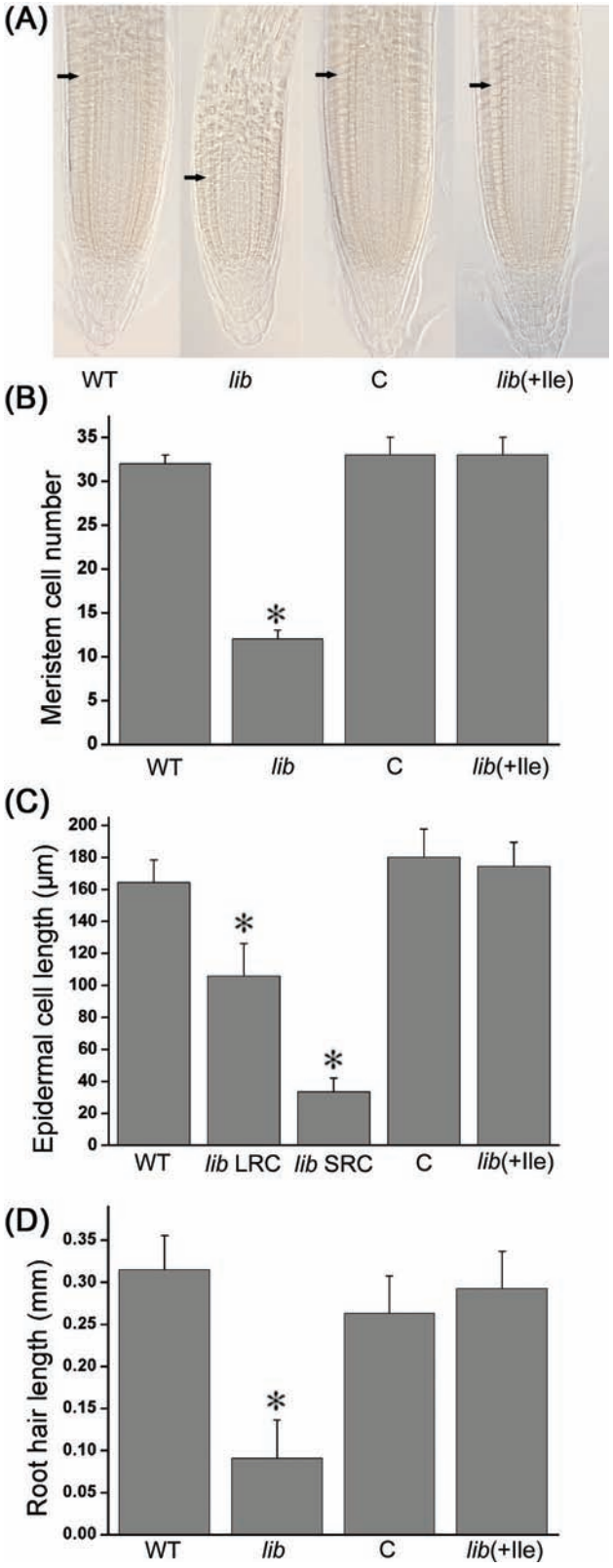

Fig. 4. Characteristics of root growth of 8-day-old seedlings of the WT, *lib*, the transgenic line of *OMR1::OMR1* (gDNA) (C), and *lib* grown on half-strength MS medium supplemented with 5 μM isoleucine [*lib*+(Ile)]. (A) Photograph of the root meristematic regions of the four genotypes. (B) The number of root meristem cells of the four genotypes. Values are means ±SE (n >20). (C) Length of root epidermal cells of the four genotypes. Values are the means ±SE of 30 seedlings (10 root epidermal cells were measured per seedling). (D) Length of root hairs of the four genotypes. Values are the means ±SE of 30 seedlings (20 root hairs were measured per seedling). In (B), (C), and (D), asterisks indicate a significant difference from the WT according to a two-sample t-test (P < 0.05). (This figure is available in colour at *JXB* online.)

TD activity was ~40% lower in the *lib* mutant than in the WT (Fig. 5A). The profiles of free amino acids in the WT, the *lib* mutant, and an *OMR1::OMR1* (gDNA) complemented line with restored mutant phenotype were then examined. As shown in Table 1, the amounts of free isoleucine in roots were ~50% lower in the *lib* mutant than in the WT. In the complemented line, the level of isoleucine was restored to that of the WT.

Next, the effect of exogenously applied isoleucine on root growth was tested. WT and *lib* mutant seeds were directly sown on half-strength MS medium supplemented with different amounts of isoleucine and grown for 8 d. The addition of isoleucine at ≥5 μM completely rescued the mutant phenotype (Fig. 5B). The degree of rescue of the mutant phenotype by addition of isoleucine was concentration dependent (Fig. 5B). Addition of phenylalanine, whose level was also decreased in the *lib* mutant, to the culture medium failed to rescue the mutant phenotype (data not shown). This indicated that the rescue effect was isoleucine specific. To confirm the effect of isoleucine further, mutant seedlings were first grown on half-strength MS medium for 7 d and then transferred to the same medium supplemented with 10 μM isoleucine. In the following 4 d, the growth rate of the primary root (Fig. 5C) and other characteristics of root growth of the *lib* mutant (Fig. 4), including the size of root meristem, length of epidermal cells, and length of root hairs, became similar to those of the WT.

Because isoleucine is an essential structural component of proteins, whether the partial deficiency in isoleucine in the *lib* mutant would affect total protein content in the *lib* mutant was deternined. The analysis of both leaves and roots showed that there was no obvious difference in total protein content between the WT and the *lib* mutant (Fig. 5D).

OMR1 is expressed in all plant organs and is present in plastids

To determine the expression patterns of the *OMR1* gene, a 2.0 kb DNA sequence upstream of its transcription start site was fused to a *GUS* reporter gene and transformed into WT plants. Forty-five independent transgenic lines were obtained, and the *OMR1::GUS* expression pattern of a representative line is shown in Fig. 6A. In the transgenic plants, the *GUS* gene was expressed in all plant organs. This is consistent with previous reports that isoleucine is synthesized in all parts of the plant (Singh and Shaner, 1995). In roots, *GUS* expression was mainly observed in vascular tissues, and no expression was detected in the meristematic region. Similarly, in cotyledons and mature leaves, *GUS* expression was strong

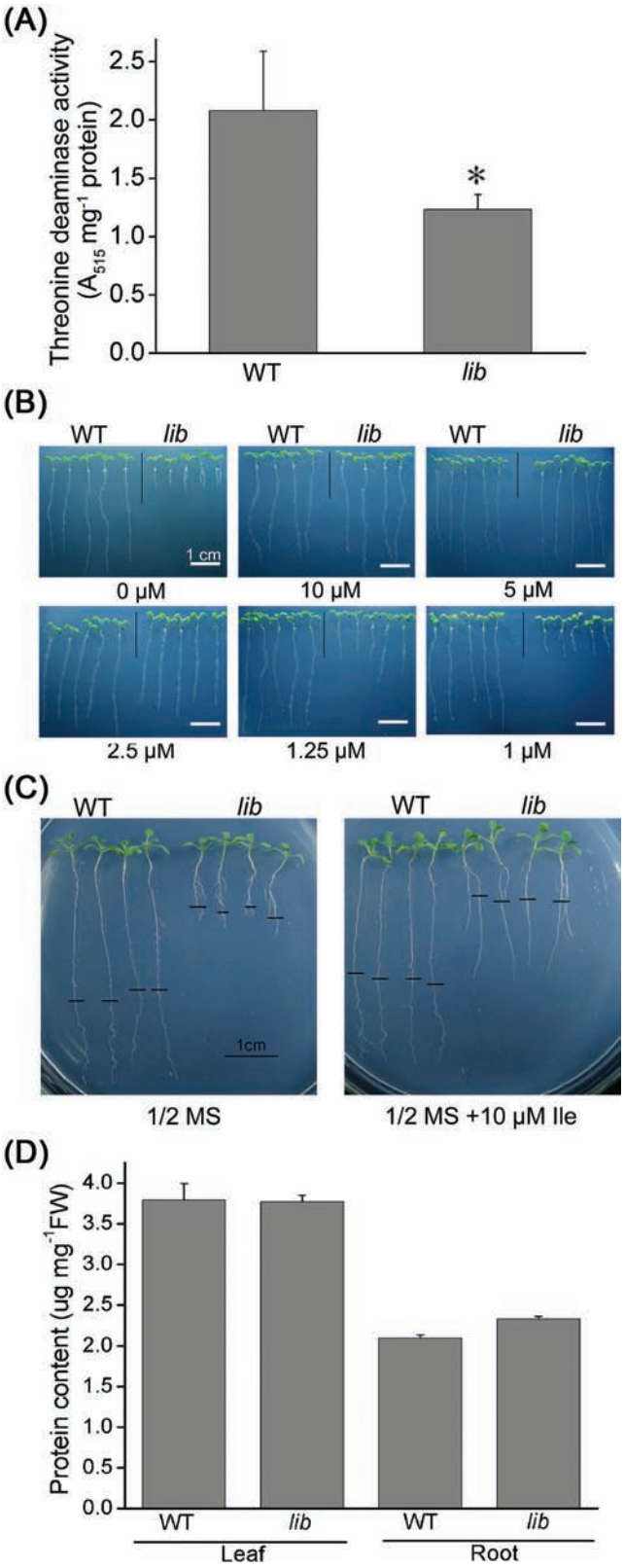

Fig. 5. Rescue of the *lib* mutant phenotype by exogenously applied isoleucine. (A) TD enzyme activity of the WT and *lib* mutant. Values are the means ±SE of four biological replicates. The asterisk indicates a significant difference according to a two-sample *t*-test ($P < 0.05$). (B) Morphology of 8-day-old seedlings of the WT and *lib* mutant grown on half-strength MS medium supplemented with different amounts of isoleucine (concentrations of isoleucine added to the medium are indicated at the bottom). (C) Effect of exogenous isoleucine when applied to WT and *lib* seedlings from 7 to 11 DAG. The seeds of the WT and *lib* were directly sown on half-strength MS medium. After 7 d, the seedlings were transferred to half-strength MS medium supplemented with isoleucine and were photographed after another 4 d of growth. The black lines indicate the positions of the root tips when the seedlings were transferred to isoleucine-containing half-strength MS medium. (D) Total protein contents in leaf and root tissues of the WT and *lib* mutant.

Table 1. Amount of free amino acids (pmol mg FW^{-1}) in the WT, lib, and the OMR1::OMR1 transgenic line.

Amino acid	Absolute amount (pmol mg FW^{-1})		
	WT	***lib***	***OMR1::OMR1***
Aspartate	117 ± 20	125 ± 31	104 ± 4
Glutamate	231 ± 10	252 ± 56	174 ± 7[a]
Glutamine	201 ± 14	261 ± 64	168 ± 6[a]
Serine	218 ± 15	265 ± 84	174 ± 7[a]
Asparagine	2980 ± 131	3160 ± 318	2130 ± 89[a]
Histidine	8.38 ± 1.09	5.03 ± 0.28	6.72 ± 2.51
Glycine	45.6 ± 7.6	59.4 ± 2.1	114 ± 26[b]
Threonine	31.6 ± 7.3	36.7 ± 2.3	26.0 ± 4.5
Arginine	26.1 ± 10.7	43.2 ± 17.8	30.1 ± 9.7
Alanine	46.8 ± 7.7	43.5 ± 16.7	47.3 ± 1.5
Tyrosine	1.93 ± 0.30	4.22 ± 2.71	2.33 ± 0.46
Cysteine	2.75 ± 0.17	3.00 ± 0.02	2.74 ± 0.07
Valine	128 ± 8	125 ± 23	90.4 ± 6.6[a]
Phenylalanine	8.03 ± 1.17	4.93 ± 1.26[a]	8.47 ± 4.21
Isoleucine	41.0 ± 4.5	20.7 ± 6.0[a]	34.6 ± 4.0
Leucine	18.5 ± 3.7	24.3 ± 7.9	43.6 ± 12.0[b]
Lysine	1.15 ± 0.53	4.89 ± 1.80[b]	6.62 ± 0.97[b]
Proline	25.6 ± 3.5	33.3 ± 8.2	35.0 ± 8.9

Values are the means ±SD of four replicates.
[a] Values significantly lower than the WT ($P < 0.05$).
[b] Values significantly higher than the WT ($P < 0.05$).

in vascular tissues but weak in interveinal regions. In stems, *GUS* expression was strongest in young, growing parts. *GUS* expression, however, was stronger in old leaves than in young leaves. In addition, *GUS* expression was observed in young pedicels and pollen grains, but not in sepals, petals, or mature siliques.

It has long been known that isoleucine is synthesized in chloroplasts but not in other cellular components (Binder, 2010). The OMR1 protein sequence is predicted to contain a transit peptide of 91 amino acids at its N-terminus for chloroplast targeting (Chlorop 1.1 Prediction Serves at http://www.cbs.dtu.dk/services/ChloroP/). For confirmation of its subcellular location, the coding sequence of *OMR1* was fused to the N-terminus of GFP and transformed into *lib* mutants under the control of the CaMV 35S promoter. The *lib* mutant phenotypes were complemented by the transformation, indicating that the 35S::OMR1–GFP fusion protein was functional (data not shown). The protoplasts from mature leaves of the transgenic plants were isolated and subjected to confocal

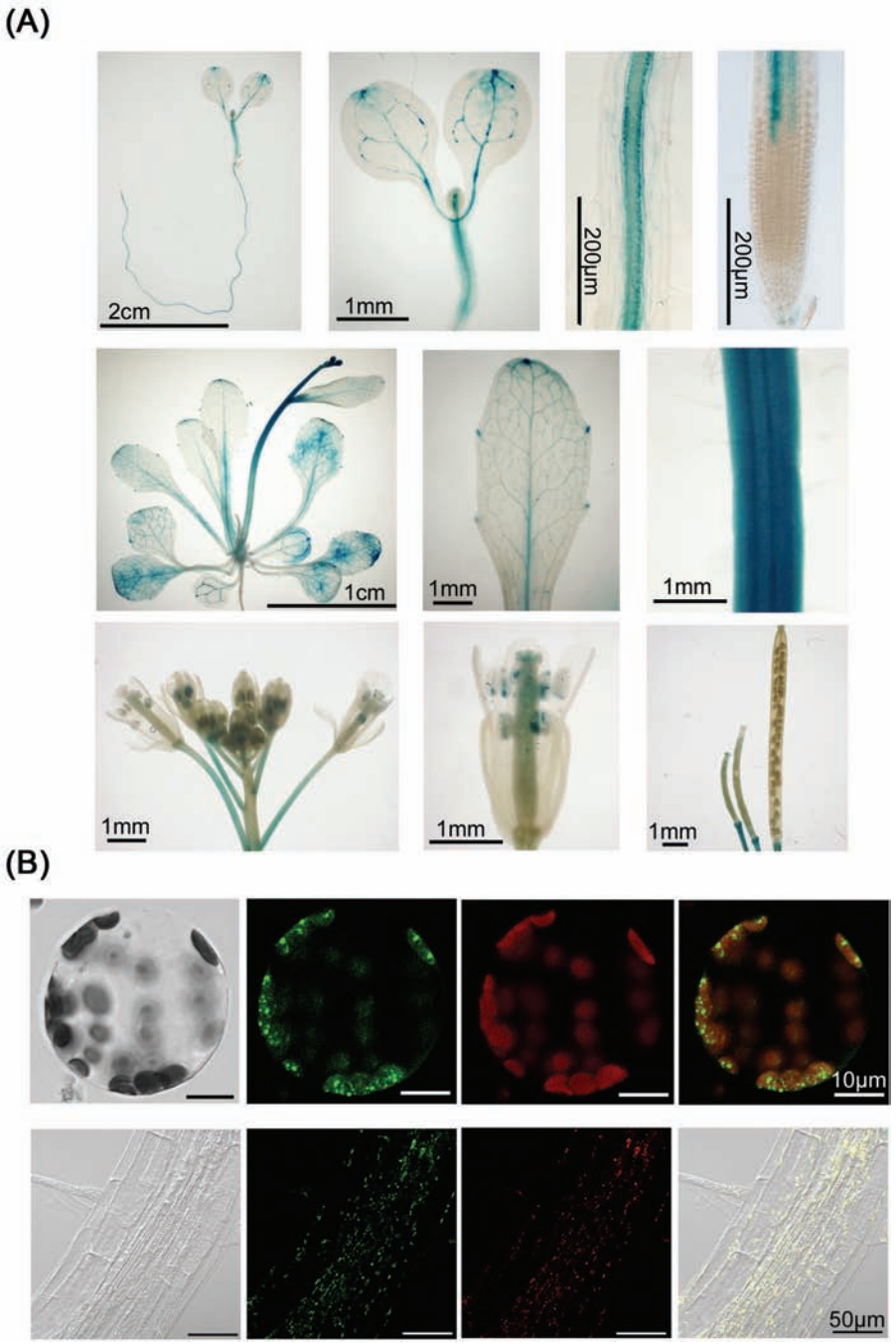

Fig. 6. The expression pattern and subcellular localization of OMR1. (A) *OMR1::GUS* expression patterns in different organs. Top row (left to right): an 8-day-old seedling; magnified views of cotyledons; root maturation zone; root tip. Middle row: aerial part of a 30-day-old plant; a leaf blade; the young part of a stem. Bottom row: an inflorescence; a fully opened flower; immature and mature siliques. (B) Subcellular localization of OMR1–GFP fusion protein. Upper row: localization of OMR1–GFP on a chloroplast in an isolated protoplast. Left to right: bright field micrograph of a protoplast; green fluorescent signal from OMR1–GFP; red autoflorescence from a chloroplast; merged micrograph of the two fluorescence images. Bottom row: co-localization of OMR1–GFP protein and pt-mCherry in the root tissues. Left to right: bright field micrograph of root tissue; green fluorescent signal from OMR1–GFP; red fluorescent signal from the plastid marker pt-mCherry; merged micrograph of the three images.

image analysis. As shown in Fig. 6B, green fluorescence signals were associated with the chloroplast. This result provided direct evidence that *Arabidopsis* TD protein is localized in leaf chloroplasts. To examine the subcellular localization of OMR1 in root tissues, the *35::OMR1-GFP* transgenic plant was crossed to a plant line carrying a plastid (pt)-specific marker gene, pt-mCherry (Nelson *et al.*, 2007). As demonstrated by the co-localization of signals of pt-mCherry and OMR1–GFP (Fig. 6B), the OMR1 protein is localized in plastids in root tissues.

Partial isoleucine deficiency affects gene expression involved in BCAA and glucosinolate metabolism

To determine how the partial deficiency of isoleucine in the *lib* mutant will affect the gene expression at the genomic level, a microarray analysis was performed comparing the gene expression profiles between the WT and *lib*. The mRNAs used for analysis were isolated from the root tissues of 8-day-old seedlings. All comparisons were made against the gene expression level of WT plants. The corrected *P*-value of <0.05 was used to select the genes for comparison, and only those genes whose expression was 2-fold higher or lower in *lib* than in the WT were used for analysis. The results indicated that expression in the *lib* mutant was up-regulated for 453 genes and down-regulated for 451 genes (Supplementary Tables S1, S2 at *JXB* online). Using the SBC Analysis program (http://sas.ebioservice.com/index.jsp), it was found that almost all the pathways that were significantly affected in the *lib* mutant are involved in amino acid and secondary metabolism (Supplementary Table S3). The significant genes over-represented in the metabolic pathways are listed in Supplementary Table S4. The expression levels of the genes that are involved in the BCAA metabolic pathway were then examined. As predicted by the SBC analysis program, the expression of two *IPMS-like* genes (At5g23010 and At5g23020; Field *et al.*, 2004; Kroymann *et al.*, 2001) increased 2.88- and 4.65-fold, respectively, and the expression of the *BCAT4* gene (At3g19710; Diebold *et al.*, 2002) increased 6.77-fold in the *lib* mutant (Fig. 7A). These three genes have also been demonstrated to participate in the chain elongation pathway in the biosynthesis of methionine-derived glucosinolates (Sønderby *et al.*, 2010). The increased expression of these three genes in *lib* was validated by quantitative real-time PCR analysis (Fig. 8). Using quantitative real-time PCR, it was also found that the increased expression of these three genes was reversed in the complemented line and in *lib* grown on isoleucine-containing MS medium (Fig. 8), supporting the view that the altered expression of these three genes in *lib* was due to a deficiency in isoleucine biosynthesis. In contrast, the expression of *BCAT2* (At1g10070; Diebold *et al.*, 2002), branched-chain α-keto dehydrogenase (BCKDH; Mooney *et al.*, 2002) E1α subunit (At1g21400), BCKDH E1β subunit (At3g13450), BCKDH E2 subunit (At3g06850), isovaleryl-CoA dehydrogenase (IVD, At3g45300; Faivre-Nitschke *et al.*, 2001), and 3-methycrotonyl-CoA carboxylase (MCCase; Song *et al.*, 1994) α subunit (At1g03090) and β subunit (At4g34030) was lower in the *lib* mutant than in the WT. The decrease in the transcript levels of these genes was moderate, but was statistically significant, ranging from 27% to 46% of the WT. The fold changes of these transcripts are indicated in Fig. 7B. BCKDH and IVD are the enzymes involved in the early steps of degradation of all three BCAAs, and MCCase catalyses the reaction toward the degradation of leucine (Fig. 7B). The decrease in the transcript levels of the genes encoding these enzymes suggested that the overall degradation activity of BCAA is reduced in *lib*.

Discussion

In this work, an *Arabidopsis* mutant that has defects in both root cell proliferation and cell expansion, but not in root cell patterning, was characterized. The phenotypes of the *lib* mutant are caused by a T-DNA insertion within the *OMR1* gene (At3g10050), which encodes a TD. In plants, TD catalyses the deamination and dehydration of threonine to produce ammonia and 2-oxobutanoate, which is the first and also the committed step in the biosynthesis of isoleucine (Binder, 2010). Complete loss of TD activity in a *Nicotiana plumbaginifolia* mutant or inhibition of TD in *Arabidopsis* and corn by herbicide results in plant death (Colau *et al.*, 1987; Szamosi *et al.*, 1994). Strong silencing of TD in *Nicotiana attenuata* also caused severely stunted growth (Kang *et al.*, 2006). Thus, complete loss or strong inhibition of TD enzyme activity might mask the specific roles of isoleucine in plant development. In the *lib* mutant used here, TD activity was 40% lower than in the WT because of the T-DNA insertion, which results in the expression of a truncated version of the OMR1 mRNA. The amounts of isoleucine in roots of the *lib* mutant were about half of those in the WT. The *lib* mutant phenotype could be rescued by application of exogenous isoleucine or by transformation with a WT *OMR1* gene, but not by supplementation with phenylalanine, whose level was also decreased in the *lib* mutant. These results support the notion that the *lib* mutant phenotype is specifically caused by a deficiency in isoleucine. Thus, the *lib* mutant provides a useful material to examine the role of isoleucine in plant development.

How does the deficiency in isoleucine impair root development? One possibility is that isoleucine may play a regulatory or signalling role in the control of root development. Previous studies have shown that various amino acid deficiencies have different effects on plant growth and development. For example, the *Arabidopsis* mutant *hpa1* has a reduced amount of histidine (Mo *et al.*, 2006). Besides having a reduced root meristem, the *hpa1* mutant also has altered QC activity and cell patterning, which were not observed in the *lib* mutant. A *gapcp* double mutant of *Arabidopsis* that produces a low level of serine has arrested primary root growth but normal lateral root growth (Muñoz-Bertomeu *et al.*, 2009). This is also different from the *lib* mutant. Another *Arabidopsis* mutant, *smo1*/*trp2-301*, which bears a defect in biosynthesis of tryptophan, has small above-ground organs but normal primary root growth (Jing *et al.*, 2009). Although tryptophan is the precursor for the biosynthesis of auxin, the *smo1*/*trp2-301* mutant phenotypes could only be rescued by exogenously applied tryptophan, but not auxin, indicating that the mutant phenotype specifically reflects a deficiency in tryptophan. Other unique phenotypes that were observed in the roots of *lib* were the alternative appearance of LRC and SRC regions as well as the regions with or without root hairs (Fig. 2). In *Arabidopsis*, biosynthesis of isoleucine is significantly slower in the light than in the dark (Coruzzi and Last, 2000). The diurnal change in the isoleucine biosynthesis rate may result in the alternative patterns of LRCs and SRCs as well as in the formation of root hairs. The distinct effects of perturbed

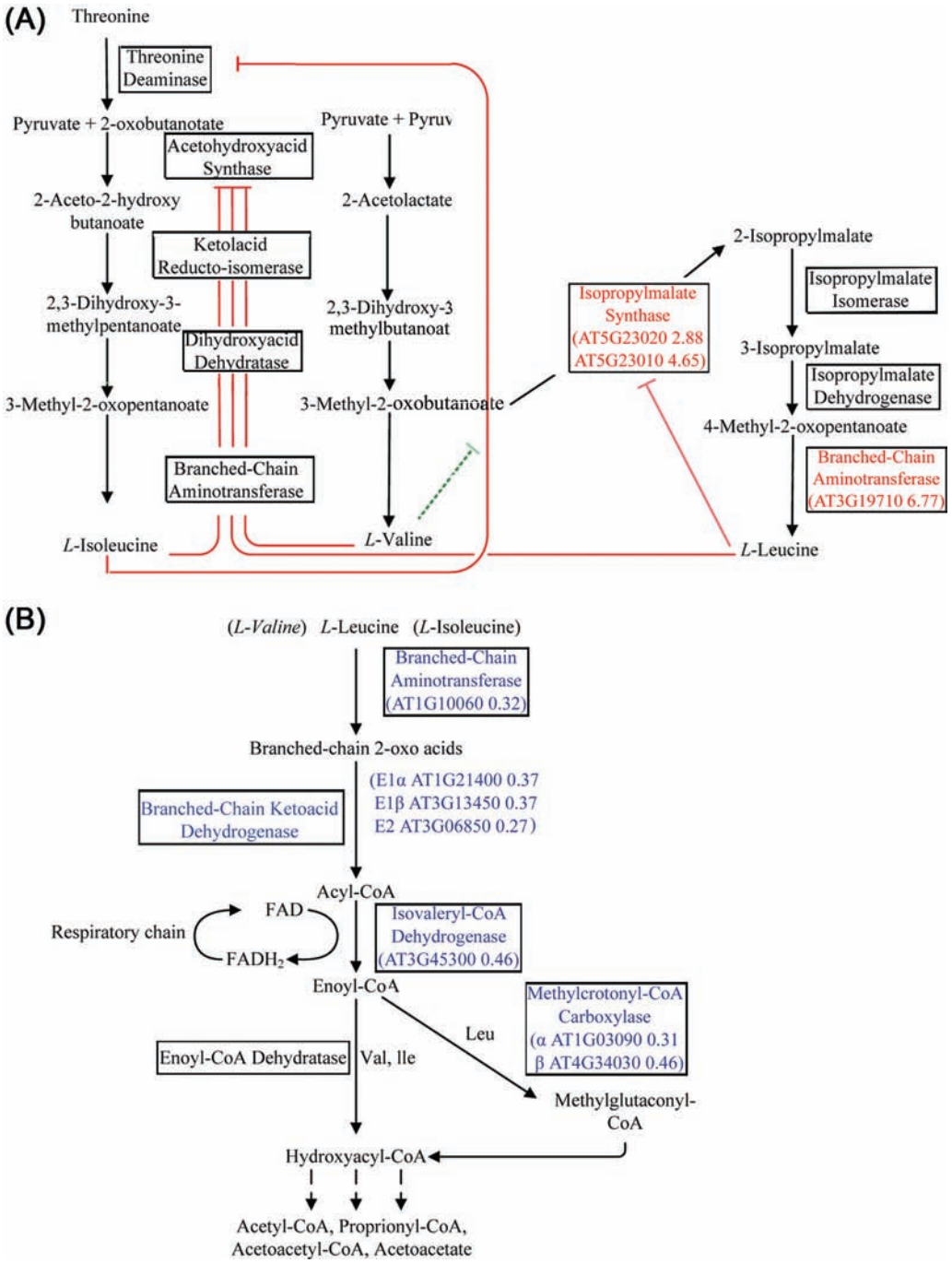

Fig. 7. The BCAA metabolic pathway. (A) The BCAA biosynthesis pathway. The substrates and enzymes catalysing each step are shown. Feedback inhibition by the end-product is indicated by a red line. The antagonistic effect of valine on the inhibition of TD by isoleucine is indicated by a green dotted line. The enzymes whose transcript level is increased in *lib* are shown in red. The numbers along the AGI gene code indicate the ratio of expression of that gene in *lib* versus the WT. (B) The BCAA degradation pathway. The substrates and enzymes catalysing each step are shown. The enzymes whose transcript level is decreased in *lib* are shown in blue. The numbers along the AGI gene code indicate the ratio of expression of that gene in *lib* versus the WT. In (A) and (B), the names of enzymes are boxed.

homeostasis of different amino acids on root development suggest that these amino acids may have regulatory roles rather than simply serving as building blocks for general protein synthesis. This notion is supported by the fact that general protein synthesis is not impaired in *lib* and *smo1/trp2-301* mutants. In plants, jasmonate (JA) is an important hormone that regulates a variety of biological processes. The most active form of JA is its conjugate with isoleucine (JA-Ile) (Thines *et al.*, 2007). Tobacco plants with a partial deficiency in isoleucine were highly susceptible to insect attack (Kang

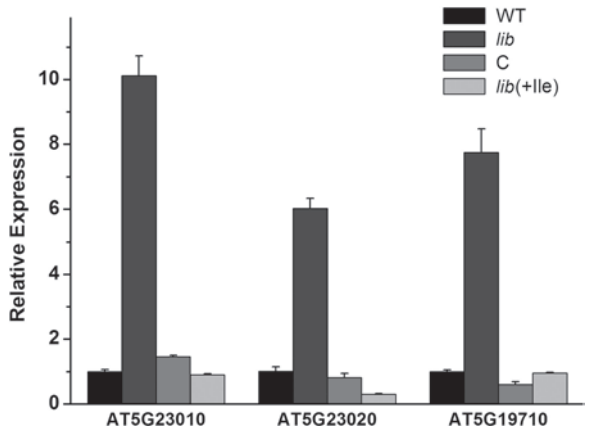

Fig. 8. Relative expression of the two *IPMS-like* genes (At5g23010 and At5g23020) and the *BCAT4* gene (At3g19710) in the WT, *lib*, a complemented line (C), and *lib* grown on half-strength MS medium supplemented with 5 μM isoleucine [*lib*(+Ile)]. Total RNAs were extracted from roots of 8-day-old seedlings, and the relative expression levels of the three genes were determined by quantitative real-time PCR. The AGI code of the genes is indicated at the bottom. The expression of the gene in the WT was set at 1.

et al., 2006). Further studies indicated that low production of isoleucine in these plants decreased the formation of JA-Ile, thus affecting the JA signalling pathway and finally reducing plant resistance to herbivore attack. The role of JA in regulating root growth has been well recognized (Wasternack, 2007). Recent research demonstrates that JA regulates auxin synthesis and transport during lateral root growth (Sun *et al.*, 2009). Thus, it is possible that the low level of isoleucine in the *lib* mutant may reduce formation of JA-Ile, which in turn affects root development through the change of the JA signalling process or the interactions with other hormones.

Considering the results obtained from this work, however, the possibility that the impairment in root development in *lib* is due to a reduction of general protein biosynthesis cannot be completely excluded. Although the total protein content in *lib* is not reduced per gram of fresh weight or per cell, it is reduced per plant. The hypothesis that the *lib* phenotype results from reduced protein synthesis is supported by the fact that, like *lib* root growth, *lib* shoot growth is also reduced on medium lacking isoleucine. The suppression of the mutant phenotypes in soil-grown *lib* plants might result from the presence of a small amount of isoleucine (derived from decomposed plants or microorganisms) in soil.

To maintain normal growth and development, plants must tightly regulate both primary and secondary metabolism, including the pathway that controls BCAA homeostasis. *Arabidopsis* has seven annotated genes encoding BCAT, and six of them are actively transcribed (Diebold *et al.*, 2002). Although it has been biochemically demonstrated that BCATs are required for the last step of biosynthesis and the first step of degradation for all three BCAAs, it is still unclear how each of these six BCATs contributes to the biosynthesis and degradation process. The present microarray analysis indicated that among these six active *BCAT* genes, only *BCAT2* (At1g10060) and *BCAT4* (At3g19710) showed significant changes of expression in the *lib* mutant. Because the partial deficiency of isoleucine in *lib* down-regulates the transcript level of *BCAT2* but up-regulates *BCAT4*, it seems unlikely that these two genes both act in either biosynthesis or degradation. Considering that the three major enzymes involved in BCAA degradation are all down-regulated in *lib* (as discussed below), it was believed that BCAT2 is involved in the first step of the BCAA degradation pathway (Fig. 7B).

Interestingly, although there are five enzymes involved in biosynthesis of isoleucine, isoleucine deficiency in *lib* did not alter transcript levels of any of the genes encoding these enzymes. Instead, the transcript levels of the genes encoding the enzymes involved in the three early steps of degradation is decreased (Fig. 7B). These enzymes include BCKDH, IVD, and MCCase. BCKDH catalyses the second step in the BCAA degradation pathway. This enzyme is a protein complex consisting of multiple subunits of E1α, E1β, E2, and E3 (Mooney *et al.*, 2002). In *lib*, the expression of the genes encoding E1α, E1β, and E2 subunits was coordinately down-regulated. Similarly, MCCase, which is involved in leucine degradation, consists of two subunits, α and β (Alban *et al.*, 1993; Song *et al.*, 1994). In the *lib* mutant, the expression of both of these subunits is decreased. The strong co-expression of E1α, E1β, and E2 subunits of BCKDH, α and β subunits of MCCase, IVD, and BCAT2 was also observed when plant cells were exposed to carbon starvation, dark, or abscisic acid (ABA) treatment (Fujiki *et al.*, 2001; Mentzen *et al.*, 2008; Urano *et al.*, 2009; Binder, 2010). Based on these results, it is proposed that in the biosynthesis pathway, isoleucine homeostasis may mainly be achieved through the regulation of enzyme activity, such as feedback control of TD activity by isoleucine, rather than through transcriptional effects. In the degradation pathway, however, the regulation of BCAA homeostasis may be achieved mainly through the alteration of the transcription of degradative enzymes.

Because BCAT4 acts on leucine but not on isoleucine or valine (Schuster *et al.*, 2006), it was speculated that BCAT4 is involved in the last step of leucine biosynthesis (Fig. 7A). Also, the increased expression of two *IPMS-like* genes (At5g23010 and At5G23020) suggested that more carbon might flow into the leucine biosynthesis pathway through the branch point from the valine biosynthesis pathway (Fig. 7A). Our analysis, however, did not detect a significant increase of leucine content in *lib* (Table 1). Instead, *BCAT4* and these two *IPMS-like* genes are well known to be involved in the chain elongation pathway in the biosynthesis of methionine-derived glucosinolates in *Arabidopsis*. This pathway starts with a deamination reaction by a BCAT that is followed by a condensation reaction catalysed by methylthioalkylmalate synthase (MAM) (Sønderby *et al.*, 2010). BCAT4 has been implicated in catalysis of the initial deamination step of methionine (Schuster *et al.*, 2006), and the products of two *IPMS-like* genes have been demonstrated to have MAM activity (Kroymann *et al.*, 2001; Field *et al.*, 2004). In addition, the expression of several other genes involved in the glucosinolate

biosynthesis pathway (Hirai *et al.*, 2007; Sawada *et al.*, 2009) was up-regulated in *lib* (Supplementary Tables S3, S4 at *JXB* online). Taken together, the partial deficiency of isoleucine in *lib* may enhance biosynthesis of methionine-derived glucosinolates rather than biosynthesis of leucine. The increased accumulation of glucosinolate in *lib*, however, requires experimental confirmation. Furthermore, because a change in glucosinolate content can affect plant growth and development (Kim *et al.*, 2004; Reintanz *et al.*, 2004; Tantikanjana *et al.*, 2004), the retarded growth of *lib* could also be due to the indirect effect resulting from the increased accumulation of glucosinolates.

Supplementary data

Supplementary data are available at *JXB* online.

Figure S1. Changes in the number of the first-order lateral roots of WT and *lib* mutants from 5 to 13 DAG.

Figure S2. The patterns of root hair development in 8-day-old WT and *lib* seedlings.

Figure S3. The expression patterns of seven cell-specific markers in the roots of 8-day-old WT and *lib* mutant seedlings.

Figure S4. The relative expression of the OMR1 gene in roots of the WT and transgenic plants.

Text S1. Methods for vector construction and plant transformation.

Table S1. The genes whose expression is up-regulated in the *lib* mutant.

Table S2. The genes whose expression is down-regulated in the *lib* mutant.

Table S3. The metabolic pathways that are perturbed in the *lib* mutant.

Table S4. The significant genes over-represented in the metabolic pathways.

Acknowledgements

We thank Dr Lijia Qu (Peking University) for providing the *Arabidopsis* T-DNA activation library; Dr Chuanyou Li (Institute of Genetics and Developmental Biology, Chinese Academy of Sciences), Dr Ben Scheres (Utrecht University, Netherlands), and the European *Arabidopsis* Stock Center for providing the GFP and GUS marker lines; and Lei Huang (Tsinghua University) for help with confocal image analysis. This work was supported by the Ministry of Science and Technology of China (grant no. 2009CB119100), the National Natural Science Foundation of China (grant no. 31170238), and the Ministry of Agriculture of China (grant no. 2011ZX08009-003-005).

References

Alban C, Baldet P, Axiotis S, Douce R. 1993. Purification and characterization of 3-methycrotonyl-coenzyme A carboxylase from higher plant mitochondria. *Plant Physiology* **102,** 957–965.

Binder S. 2010. Branched-chain amino acid metabolism in *Arabidopsis thaliana*. *The Arabidopsis Book* **8**: e0137. doi:10.1199/tab.0137.

Colau D, Negrutiu I, Van Montagu M, Hernalsteens JP. 1987. Complementation of a threonine dehydratase-deficient Nicotiana plumbaginifolia mutant after Agrobacterium tumefaciens-mediated transfer of the *Saccharomyces cerevisiae* ILV1 gene. *Molecular and Cellular Biology* **7,** 2552–2557.

Colón-Carmona A, You R, Haimovitch-Gal T, Doerner P. 1999. Spatio-temporal analysis of mitotic activity with a labile cyclin–GUS fusion protein. *The Plant Journal* **20,** 503–508.

Coruzzi C, Last R. Amino acids. In: Buchana B, Gruissem W, Jones R, eds. *Biochemistry & molecular biology of plants*. Rockville, MD: American Society of Plant Biologists, 358–363.

de Kraker JW, Luck K, Textor S, Tokuhisa JG, Gershenzon J. 2007. Two *Arabidopsis* genes (*IPMS1* and *IPMS2*) encode isopropylmalate synthase, the branchpoint step in the biosynthesis of leucine. *Plant Physiology* **143,** 970–986.

Diebold R, Schuster J, Däschner K, Binder S. 2002. The branched-chain amino acid transaminase gene family in *Arabidopsis* encodes plastid and mitochondrial proteins. *Plant Physiology* **129,** 540–550.

Faivre-Nitschke SE, Couée I, Vermel M, Grienenberger JM, Gualberto JM. 2001. Purification, characterization and cloning of isovaleryl-CoA dehydrogenase from higher plant mitochondrial. *European Journal of Biochemistry* **268,** 1332–1339.

Field B, Cardon G, Traka M, Botterman J, Vancanneyt G, Mithen R. 2004. Glucosinolate and amino acid biosynthesis in *Arabidopsis*. *Plant Physiology* **135,** 828–839.

Fujiki Y, Ito M, Nishida I, Watanabe A. 2001. Leucine and its keto acid enhance the coordinated expression of genes for branched-chain amino acid catabolism in *Arabidopsis* under sugar starvation. *FEBS Letters* **499,** 161–165.

Halgand F, Wessel PM, Laprévote O, Dumas R. 2002. Biochemical and mass spectrometric evidence for quaternary structure modifications of plant threonine deaminase induced by isoleucine. *Biochemistry* **41,** 13767–13773.

Hirai MY, Sugiyama K, Sawada Y, *et al.* 2007. Omics-based identification of Arabidopsis Myb transcription factors regulating aliphatic glucosinolate biosynthesis. *Proceedings of the National Academy of Sciences, USA* **104,** 6478–6483.

Jefferson RA, Kavanagh TA, Bevan MW. 1987. GUS fusions: beta-glucuronidase as a sensitive and versatile gene fusion marker in higher plants. *EMBO Journal* **6,** 3901–3907.

Jing Y, Cui D, Bao F, Hu Z, Qin Z, Hu Y. 2009. Tryptophan deficiency affects organ growth by retarding cell expansion in *Arabidopsis*. *The Plant Journal* **57,** 511–521.

Kang JH, Wang L, Giri A, Baldwin IT. 2006. Silencing threonine deaminase and JAR4 in *Nicotiana attenuata* impairs jasmonic acid-isoleucine-mediated defenses against *Manduca sexta*. *The Plant Cell* **18,** 3303–3320.

Kim JH, Durrett TP, Last RL, Jander G. 2004. Characterization of the *Arabidopsis* TU8 glucosinolate mutation, an allele of TERMINAL FLOWER2. *Plant Molecular Biology* **54,** 671–682.

Kimball SR, Jefferson LS. 2006. New functions for amino acids: effects on gene transcription and translation. *American Journal of Clinical Nutrition* **83,** 500s–507s.

Kroymann J, Textor S, Tokuhisa JG, Falk KL, Bartram S, Gershenzon J, Mitchell-Olds T. 2001. A gene controlling variation in *Arabidopsis* glucosinolate composition is part of the methionine chain elongation pathway. *Plant Physiology* **127,** 1077–1088.

Levine B, Klionsky DJ. 2004. Development by self-digestion: molecular mechanisms and biological functions of autophagy. *Developmental Cell* **6,** 463–477.

Liu YG, Mitsukawa N, Oosumi T, Whittier RF. 1995. Efficient isolation and mapping of Arabidopsis thaliana T-DNA insert junctions by thermal asymmetric interlaced PCR. *The Plant Journal* **8,** 457–463.

Mentzen WI, Peng J, Ransom N, Nikolau BJ, Wurtele ES. 2008. Articulation of three core metabolic processes in Arabidopsis: fatty acid biosynthesis, leucine catabolism and starch metabolism. *BMC Plant Biology* **8,** 76.

McCourt JA, Duggleby RG. 2006. Acetohydroxyacid synthase and its role in the biosynthetic pathway for branched-chain amino acids. *Amino Acids* **31,** 173–210.

Meijer AJ, Dubbelhuis PF. 2004. Amino acid signalling and the integration of metabolism. *Biochemcal and Biophysical Research Communications* **313,** 397–403.

Mo X, Zhu Q, Li X, Li J, Zeng Q, Rong H, Zhang H, Wu P. 2006. The *hpa1* mutant of *Arabidopsis* reveals a crucial role of histidine homeostasis in root meristem maintenance. *Plant Physiology* **141,** 1425–1435.

Mooney BP, Miernyk JA, Randall DD. 2002. The complex fate of keto acids. *Annual Review of Plant Biology* **53,** 357–375.

Mourad G, Emerick R, Smith A. 2000. Molecular cloning and sequencing of a cDNA encoding an isoleucine feedback insensitive threonine dehydratase/deaminase of *Arabidopsis thaliana* line GM11b Accession No. (AF177212) (PGR00-020). *Plant Physiology* **122,** 619.

Mourad G, King J. 1995. L-*O*-Methylthreonine-resistant mutant of *Arabidopsis* defective in isoleucine feedback-regulation. *Plant Physiology* **107,** 43–52.

Muñoz-Bertomeu J, Cascales-Miñana B, Mulet JM, Baroja-Fernández E, Pozueta-Romero J, Kuhn JM, Segura J, Ros R. 2009. Plastidial glyceraldehyde-3-phosphate dehydrogenase deficiency leads to altered root development and affects the sugar and amino acid balance in *Arabidopsis*. *Plant Physiology* **151,** 541–558.

Nelson BK, Cai X, Nebenführ A. 2007. A multicolored set of *in vivo* organelle markers for co-localization studies in *Arabidopsis* and other plants. *The Plant Journal* **51,** 1126–1136.

Noutoshi Y, Ito T, Shinozaki K. 2005. *ABINO AND PALE GREEN 10* encodes BBMII isomerase involved in histidine biosynthesis in *Arabidopsis thaliana*. *Plant and Cell Physiology* **46,** 1165–1172.

Qin G, Kang D, Dong Y, *et al.* 2003. Obtaining and analysis of flanking sequences from T-DNA transformants of *Arabidopsis*. *Plant Science* **165,** 941–949.

Reintanz B, Lehnen M, Reichelt M, Gershenzon J, Kowalczyk M, Sandberg G, Goddea M, Uhl R, Palme K. 2004. *bus*, a bushy Arabidopsis CYP79F1 knockout mutant with abolished synthesis of short-chain aliphatic glucosinolates. *Plant Molecular Biology* **54,** 671–682.

Sawada Y, Kuwahara A, Nagano M, Narisawa T, Sakata A, Saito K, Hirai MY. 2009. Omics-based approaches to methionine side chain elongation in Arabidopsis: characterization of the genes encoding methylthioalkylmalate isomerase and methylthioalkylmalate dehydrogenase. *Plant and Cell Physiology* **50,** 1181–1190.

Schuster J, Knill T, Reichelt H, Gershenzon J, Binder S. 2006. BRANCHED-CHAIN AMINOTRANSFERASE 4 is part of the chian elongation pathway in the biosynthesis of methionine-derived glucosinolates in *Arabidopsis. The Plant Cell* **18,** 2664–2279.

Singh BK, Shaner DL. 1995. Biosynthesis of branched chain amino acids: from test tube to field. *The Plant Cell* **7,** 935–944.

Sønderby IE, Geu-Flores F, Barbara A, Halkier B. 2010. Biosynthesis of glucosinolates—gene discovery and beyond. *Trends in Plant Science* **15,** 283–290.

Song J, Wurtele ES, Nikolau BJ. 1994. Molecular cloning and characterization of the cDNA coding for the biotin-containing subunit of 3-methycrotonoyl-CoA carboxylase: identification of the biotin carboxylase and biotin-carrier domain. *Procedings of the National Academy of Sciences, USA* **91,** 5779–5783.

Sun J, Xu Y, Ye S, *et al.* 2009. Arabidopsis *ASA1* is important for jasmonate-mediated regulation of auxin biosynthesis and transport during lateral root formation . *The Plant Cell* **21,** 1495–1511.

Szamosi IT, Shaner DL, Singh BK. 1994. Inhibition of threonine dehydratase is herbicidal. *Plant Physiology* **106,** 1257–1260.

Tantikanjana T, Mikkelsen MD, Hussain M, Halkier BA, Sundaresan V. 2004. Functional analysis of the tandem-duplicated P450 genes SPS/BUS/CYP79F1 and CYP79F2 in glucosinolate biosynthesis and plant development by Ds transposition-generated double mutants. *Plant Physiology* **135,** 840–488.

Thines B, Katsir L, Melotto M, Niu Y, Mandaokar A, Liu G, Nomura K, He SY, Howe GA, Browse J. 2007. JAZ repressor proteins are targets of the SCF(COI1) complex during jasmonate signalling. *Nature* **448,** 661–665.

Urano K, Maruyama K, Ogata Y, *et al.* 2009. Characterization of the ABA-regulated global responses to dehydration in *Arabidopsis* by metabolomics. *The Plant Journal* **57,** 1065–1078.

Walch-Liu P, Liu L, Remans T, Tester M, Forde BG. 2006. Evidence that L-glutamate can acts as an exogenous signal to modulate root growth and branching in *Arabidopsis thaliana*. *Plant and Cell Physiology* **47,** 1045–1057.

Wasternack C. 2007. Jasmonates: an update on biosynthesis, signal transduction and action in plant stress response, growth and development. *Annals of Botany* **100,** 681–697.